The importance of seasonal differences in the cellulose microfibril angle in softwoods in determining acoustic properties

R. HORI
Wood Research Institute, Kyoto University, Uji, Kyoto 611-0011, Japan

M. MÜLLER*
European Synchrotron Radiation Facility, B. P. 220, F-38043, Grenoble Cedex, France

U. WATANABE
Department of Precision Engineering, Faculty of Engineering, Chiba Institute of Technology, Narashino, Chiba 275-0016 Japan

H. C. LICHTENEGGER, P. FRATZL
Erich Schmid Institute for Material Science and Metal Physics Institute, University of Leoben, Jahnstraße 12, A-8700 Leoben, Austria

J. SUGIYAMA†
Wood Research Institute, Kyoto University, Uji, Kyoto 611-0011, Japan
E-mail: junjis@kuwri.kyoto-u.ac.jp

The influence of the micro- and mesoscopic structure of wood cell walls on the acoustic properties of softwood was investigated in a synchrotron X-ray microbeam diffraction experiment with particular attention to the seasonal differences in crystallographic features. A multiple regression analysis was performed for data from 12 different softwood species in order to determine the dependence of longitudinal relative Young's modulus (E/ρ) and loss tangent ($\tan\delta$) on seasonal cellulose microfibril angles (MFAs), crystal width of cellulose microfibrils etc. We conclude that a low MFA in both latewood and earlywood yields high E/ρ and low $\tan\delta$, which is an attribute of wood used as violin or piano soundboards. Among the softwood species we characterized Sitka spruce best fits this criterion.

1. Introduction

Among a great variety of softwood species, the wood of Norway spruce (*Picea abies*) and more recently Sitka spruce (*Picea sitchensis*) have been shown to be superior for violin and piano soundboards [1–3]. Many studies have been devoted to understanding the unique acoustic properties of those two species [1–4], however, their origin is not clear yet.

One possible explanation might be found in the micro- and mesoscopic structure of wood cell walls. The architecture of softwood is rather simple, especially when compared to hardwood. 95% of the wood is made of longitudinal elements, and most of those are fibers. Cell walls have a multiple layer structure with a primary (P) and up to three secondary walls (S_1, S_2, S_3), which are distinguished by the degree of order and orientation of cellulose microfibrils [5]. The crystalline microfibrils are embedded in an amorphous matrix made from cellulose, hemicellulose and liginin. Of these layers, the thickest wall layer (up to 80% of the total thickness) is the central part of the secondary wall (S_2). Thus, the inclination angle of the cellulose microfibrils with respect to the longitudinal cell axis, particularly in the S_2 layer, the so-called microfibril angle (MFA), is of major importance for the mechanical and the closely related acoustic properties of wood [4].

The velocity of sound v_s (and, therefore, the acoustic properties) is directly related to the specific elastic modulus E/ρ, ($v_s = (E/\rho)^{0.5}$). E/ρ can thus be used as an index for the assessment of the acoustic properties. A high longitudinal elastic modulus E is associated with low MFA according to Refs. [6, 7]. The second important parameter is the internal damping of wood, expressed as the loss tangent ($\tan\delta$), which can be estimated from dynamic mechanical measurements. Tan δ is highly correlated with E/ρ [1, 2].

Although the MFA varies in an annual ring of a tree from earlywood (low density) to latewood (high

Present Address: Institut für Experimentelle und Angewandte Physik der Christian-Albrechts-Universität zu Kiel, D-24098 Kiel, Germany.
†Author to whom all correspondence should be addressed.

density) and is indeed species-specific, the mechanical properties of a given piece of wood are generally treated only as averaged values. However, it seems reasonable to include the individual MFAs from early- and latewood in experimental studies as they might also cause differences in the mechanical/acoustic properties of softwoods. There are several methods of investigating this seasonal variation of MFA, such as light microscopy [8] or small-angle X-ray scattering [9–11]. Among those methods, the novel X-ray microbeam scanning method, using a synchrotron radiation source, has the advantage of measuring the MFA variation in an annual ring with a position resolution of a few micrometers (i.e., smaller than an individual wood fiber). One example is reported by Lichtenegger *et al.* [12], where an MFA map of a cross section of spruce latewood could be obtained with microscopic resolution.

In this work we employed the X-ray microbeam scanning technique to examine seasonal changes in the crystallographic features of 12 softwoods. Some acoustic properties of the corresponding samples were measured in dynamic bending tests in the laboratory. A multiple regression analysis was carried out to determine the relationship between the crystallographic and anatomical features and the assumed determinators of the acoustic properties in order to elucidate why spruce wood is superior for musical instruments.

2. Material and methods

2.1. Samples

12 softwood samples were used throughout this study. Among them, 6 species were taken from *Picea* and the other 6 species were selected from a wood collection of our institute. *Picea sitchensis* was kindly supplied by Professor Norimoto, Kyoto University. *P. likiangasis, P. complanata, P. purpurea*, from mainland China were the kind gift from Emeritus Professor Okano of the University of Tokyo.

2.2. Measurements of physical properties

Rectangular specimens, with dimensions of 30 mm (longitudinal) × 10 mm (radial) × 1 mm (tangential), were prepared from each wood block sample as shown in Table I. The samples were conditioned at 20°C and 60% relative humidity, before and during the measurements. The specific Young's modulus (E/ρ) and flexural internal friction ($\tan\delta$) in the longitudinal direction were measured by a free-free flexural vibration method [13].

2.3. X-ray measurements

Radial sections (20 μm thick) for the X-ray experiment were cut from an air-dried block using a sliding microtome. The thickness, being smaller than the average tangential cell dimension, ensured that the samples contained only double adjacent radial cell walls from neighbouring cells (i.e., the sequence S_3 to S_1, P, middle lamella, P, S_1 to S_3) but not another wall on the other side of the lumen of a cell. The sections were mounted on one-hole Cu-grids (opening 1.5 mm in diameter). They were carefully glued to the grid to include both earlywood and latewood for the analysis.

TABLE I A summary of anatomical, physical and crystallographical features obtained from 12 softwood species. Number of samples from each specimen varies from 10 to 200

Sample name	Ring number	Physical properties		Crystal width (nm)			Average MFA (degree)		Ratio of MFAs	Annual ring	Proportion of
		E/ρ (GPa)	$\tan\delta$ ($\times 10^{-2}$)	EW	LW	Average	EW	LW	LW/EW	width (mm)	latewood (%)
Picea	–	26.0	0.70	3.4	3.4	3.4	6.5	5.3	0.83	0.88	8
sitchensis	–	33.0	0.73	3.4	3.3	3.4	6.0	5.2	0.86	1.39	5
	–	30.6	0.76	3.8	3.1	3.5	11.6	5.3	0.45	1.39	8
P. likiangasis	40th	30.2	0.80	3.6	3.4	3.5	6.5	6.2	0.96	1.84	13
	100th	31.8	0.76	3.8	3.7	3.8	8.4	5.3	0.62	1.06	19
	200th	26.6	0.81	3.8	3.8	3.8	25.6	6.7	0.26	0.33	19
P. complanata	30th	26.2	0.76	3.1	3.5	3.2	10.1	5.5	0.54	2.62	27
	50th	24.2	0.82	3.6	3.5	3.5	19.3	19.0	0.98	1.94	52
	110th	21.2	0.82	3.5	3.6	3.5	32.0	10.4	0.32	1.87	47
P. purpurea	80th	18.7	0.96	2.1	2.1	2.1	17.7	16.4	0.92	1.66	26
	130th	29.1	0.78	3.9	3.9	2.9	10.7	5.4	0.50	1.29	31
	190th	26.7	0.79	3.9	3.8	3.9	14.6	7.0	0.48	1.26	28
P. glehni	–	32.2	0.57	3.8	3.5	3.7	9.7	5.9	0.60	0.99	15
P. jazoensis	–	34.7	0.66	3.8	3.6	3.8	8.5	3.7	0.43	0.93	15
Abies sachalinensis	–	26.2	0.59	3.8	3.7	3.7	19.5	10.9	0.56	3.04	7
Chamaecyparis pisifera	–	28.9	0.56	3.9	3.6	3.8	5.9	3.3	0.55	0.91	11
Cryptomeria japonica	–	23.8	0.64	4.0	3.9	3.9	20.0	8.5	0.42	1.91	17
Cunninghamia konishiki	–	28.1	0.50	3.9	3.9	3.9	6.9	4.6	0.67	0.65	18
Pinus densiflora	–	26.0	0.72	3.8	3.6	3.7	14.8	5.5	0.37	4.18	46
Thujopsis dolabrata	–	27.0	0.64	4.1	3.7	4.0	9.2	4.5	0.49	0.49	14

–: Annual ring number was unknown.

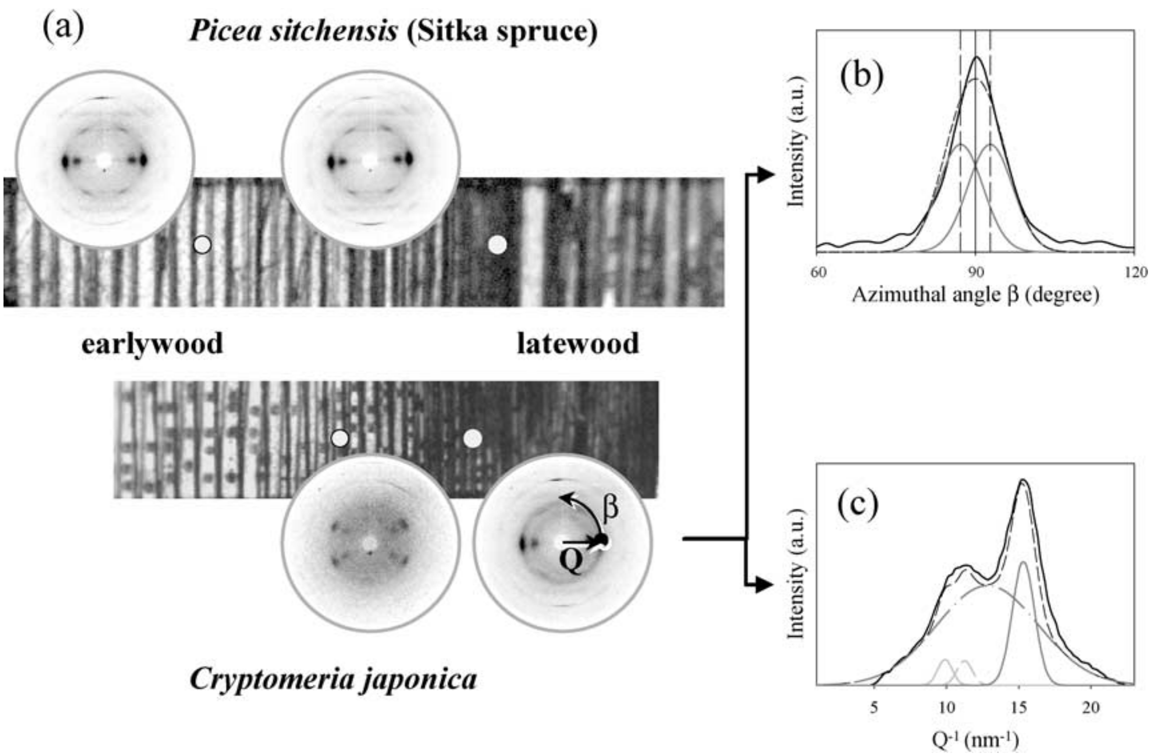

Figure 1 (a) Optical sample images and diffraction diagrams. (b) Azimuthal distribution plot from (004) plane. Solid line is direction of cell axes. MFA could be obtained from degree between cell axes and dash line. (c) Radial integration from diffraction. It was divided into four peaks ($1\bar{1}0$, 110, 200, amorphous).

The X-ray microbeam diffraction experiments were performed using the Microfocus Beamline (ID13) of the European Synchrotron Radiation Facility (ESRF, Grenoble, France). The beam was focused to 2 μm diameter by a glass capillary: the wavelength was $\lambda = 0.78$Å. The specimen was put onto a high–precision x–y gantry and could be monitored using a video microscope. Diffraction patterns were recorded with an image–intensified CCD detector (Photonics Science; distance to sample 46 mm) within 24 s accumulation time at each position. In most cases, 10 to 20 diagrams were taken from each earlywood and latewood area. In some cases, the diagrams were taken in an extended scan with a 2 μm step size from earlywood to latewood.

Fig. 1a shows a typical sample image together with X-ray microdiffraction diagrams, from which intensity profiles (Fig. 1b and c) were obtained using the computer program FIT2D [14]. Fig. 1b is an azimuthal intensity distribution ($I(\beta)$, where the azimuth angle $\beta = 90^\circ$ corresponds to the meridional direction of the diffraction diagram: solid line in Fig. 1b) integrated over a narrow radial range of the wave vector transfer Q, ($Q = 4\pi/\lambda \sin\theta$, where 2θ is the scattering angle) of the 200 reflection ($Q_{200} = 1.57$Å^{-1}). In the analysis, two Gaussian functions centered at $90^\circ \pm \Delta\beta$ were fitted to the experimental curve by a least square routine. The two maxima on the azimuth arise from the two sides of the double radial wall having opposite orientations of the microfibrils. Therefore, $\Delta\beta$ (dashed lines in Fig. 1b) corresponds to the microfibril angle (MFA). Fig. 1c is a radial integration $I(Q)$, where each profile was fitted with three Bragg peaks of crystalline cellulose I ($1\bar{1}0$, 110, 200 in the notation of [15]) and an amorphous background by a least-square program. A lower limit for the crystal width was estimated from the radial broadening of the 200 reflection by using the Scherrer formula [16].

2.4. Annual ring width and proportion of latewood

20 μm sections were prepared using a sliding microtome and stained with safranin. The images were captured using an optical microscope equipped with a CCD camera. Annual ring width and proportion of latewood were analyzed using the NIH image program. Cells were classified as latewood using Mork's definition [17].

2.5. Mathematical analysis

Statistical analysis was carried out to establish possible relationships between mechanical properties and crystallographic and anatomical features. Multiple linear regression analysis was performed using the SPSS software (SPSS Inc.) running on a PC. E/ρ and $\tan\delta$ were set as criterion variables and all other parameters were used as potential predictor variables.

3. Results and discussion

The experimental results for the 12 investigated softwood samples are summarized in Table I. For some species, samples from different annual rings were taken. Specific Young's modulus (E/ρ) and loss tangent ($\tan\delta$) where determined in acoustic tests. The X-ray microdiffraction experiments yielded values for the crystal width and microfibril angle (MFA) for both early- and latewood (EW, LW). The annual ring width and the proportion of latewood therein are from optical microscopy.

In the following, we will first discuss some of the X-ray results and then proceed to a statistical analysis of the data in order to determine correlations between structural and acoustic properties.

3.1. Crystal width

Using X-ray diffraction, Lee [18] suggested that the crystallinity of wood pulp from latewood is significantly higher than that from earlywood. More recently, however, Hult *et al.* [19] investigated chemical pulps by using CP/MAS^{13}C-NMR and came to the opposite conclusion. At first sight, our values for the crystal width in earlywood seem consistently larger those in latewood (Table I). However, using a statistical t-test, this difference was found to be insignificant in most of the specimens. Therefore, the averaged value of the crystal width was used for the further statistical analyse.

In addition, a considerable variation in crystal width between species was noticeable. Values range from ≈2 nm in *P. purpurea* (80th annual ring) to ≈4 nm in *T. dolabrata*. These differences seem, however, partly to relate to the age of the specimen.

3.2. Microfibril angle (MFA)

Interestingly, there was a clear seasonal difference in the microfibril angles (Table I), which is, in addition, individual softwood species [20, 21]. The ratio of latewood and earlywood MFAs in *Picea* is close to unity, which means there is only a small difference between them. However, this ratio is much smaller than 1 for other species. Especially there is a clear trend of very low MFA ratios in the species having distinct seasonal differences in anatomical features (e.g., color, density), such as *C. japonica, A. firma, P. densiflora*.

A number of articles conclude that MFA and E/ρ have a negative correlation [4, 6, 7]. Our results seem to support this idea, in that a lower MFA is associated with a higher E/ρ. Furthermore, since many of the previous works dealt with an averaged MFA value for a given specimen, our finding of low MFA in both earlywood and latewood for *Picea* species could shed some light on *Picea*'s particular suitability as an acoustic material.

A high MFA in earlywood compared to that in latewood increases the inhomogeneity of E/ρ and, therefore, of the velocity of sound in the radial direction, i.e., across the annual ring. The *radial* Young's modulus E_r (in contrast to the longitudinal one) increases with increasing MFA, since the microfibrils are lying more parallel to the radial direction in the case of high MFA. Therefore, earlywood with a high MFA (high E_r) and naturally low density, ρ, would be expected to give a high value of the ratio E_r/ρ, whereas for latewood it would be very small (low MFA = low E_r; high density). A very similar MFA in early- and latewood helps to reach more similar values of the velocity of sound in radial direction. This homogeneity might also be in favor of good acoustic properties.

3.3. Statistical data analysis

Since the factors governing acoustic properties are complex and cooperative, statistical analysis might provide some clues to the dependence on structural factors and their possible contributions to the target (acoustic) properties. In this study we therefore employed a multiple linear regression analysis, choosing crystallographic and anatomical features as criterion variables and E/ρ and $\tan\delta$ as prediction variables.

A correlation matrix of the criterion variables is shown in Table II. The variables are abbreviated as CW_{av} (average crystal width), MFA_{LW} (MFA in latewood), MFA_{EW} (MFA in earlywood), MFA_{LW}/MFA_{EW} (ratio between latewood and earlywood MFAs), W_{an} (annual ring width), P_{LW} (proportion of latewood). The variables highly correlated with each other were omitted as unnecessary before multiple regression analysis. Comparing the correlation coefficients, MFA_{EW}, MFA_{LW} and P_{LW} have a strong negative correlation with E/ρ whereas CW_{av} and MFA_{LW} have great influence on $\tan\delta$. Among the variables related to microfibril angles, the ratio MFA_{LW}/MFA_{EW} has a strong correlation with MFA_{EW} but less influence on the physical properties. We eliminated MFA_{LW}/MFA_{EW}, and selected the following criterion variables for further analysis: CW_{av}, MFA_{LW}, MFA_{EW}, W_{an} and P_{LW}.

A backward elimination was applied for processing, where the least useful criterion variable was removed at each step. A multiple correlation coefficient, R, is an index of apparent quality of model fitting, but R tends to be optimized simply due to increases in the number of criterion variables. The adjusted R value [22] takes this into account and was therefore used for final judgement fitting.

TABLE II Correlations among crystallographic and morphological features and physical properties

	CW_{av}	MFA in LW	MFA in EW	LW/EW	W_{an}	P_{LW}	E/ρ	$\tan\delta$
CW_{av}	1.000							
MFA_{LW}	−0.443*	1.000						
MFA_{EW}	−0.075	0.543*	1.000					
MFA_{LW}/MFA_{EW}	−0.321	0.359	−0.488*	1.000				
W_{an}	−0.131	0.301	0.270	−0.073	1.000			
P_{LW}	−0.130	0.482*	0.539*	−0.180	0.460*	1.000		
E/ρ	0.389	−0.656*	−0.669*	0.022	−0.310	−0.519*	1.000	
$\tan\delta$	−0.661*	0.509*	0.402	0.200	0.146	0.453*	−0.429	1.000

* The correlation coefficient is significant at the 0.05 level (both sided test).

CW_{av}: Average crystal width, MFA_{LW}: MFA in latewood, MFA_{EW}: MFA in earlywood, MFA_{LW}/MFA_{EW}: ratio between MFAs in latewood and earlywood, W_{an}: annual ring width, P_{LW}: proportion of latewood.

TABLE III Standardized coefficients β

	E/ρ	$\tan\delta$
CW_{av} [a]	0.234	−0.609
MFA_{LW} [a]	−0.280	
MFA_{EW} [a]	−0.502	0.246
P_{LW}^{a}		0.213

[a] Abbreviated as in Table II.

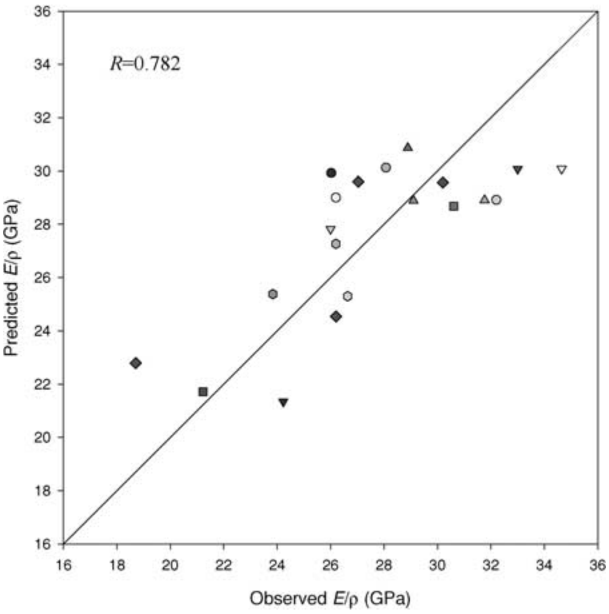

Figure 2 Multiple regression analysis plots. Criterion variable; E/ρ, predictor variable; average crystal width (CW_{av}) MFA in earlywood (MFA_{EW}) and latewood (MFA_{LW}). ● *P. sitchensis* no. 1, ▼ no. 5, ■ no. 8, ◆ *P. likiangasis* 40th, ▲ 100th, ● 200th, ● *P. complanata* 30th, ▼ 50th, ■ 110th, ◆ *P. purpurea* 80th, ▲ 130th, ● 190th, ○ *P. glehni*, ▽ *P. jazoensis*, ◆ *A. firma*, ▲ *Chamaecyparis pisifera*, ● *Cryptomeria japonica*, ● *Cunninghamia konishiki*, ▽ *Pinus densiflora*, ◆ *Thujopsis dolabrata*.

The multiple linear regression plot of E/ρ is shown in Fig. 2, and the resulting standardized coefficients, β, for the criterion variables are summarized in Table III. The plot shows the predicted values are more or less concentrated on the line of Predicted E/ρ = Observed E/ρ, giving a multiple correlation of $R = 0.782$. As in Table III, CW_{av}, MFA_{EW} and MFA_{LW} were found to be useful criterion variables, with MFA_{EW} appearing to have the largest contribution. In summary, E/ρ has negative relationships with MFA_{EW} and MFA_{LW} and a positive one with CW_{av}. Kubojima *et al.* [4] reported the same trends for MFAs and a positive relationship between "crystallinity" and E/ρ. If the term "crystallinity" implies a similar physical meaning to CW_{av}, then this finding is consistent with our results.

Fig. 3 shows the multiple regression plot of $\tan\delta$ ($R = 0.773$). The criterion variables were found to be CW_{av}, MFA_{EW}, P_{LW}. Tan δ has a positive correlation with MFA_{EW} and P_{LW} and a negative one with CW_{av} (Table III). In this case, the average crystal width, CW_{av}, seems to influence the value of $\tan\delta$ most. This correlation of CW_{av} with $\tan\delta$ has also been reported elsewhere in terms of crystallinity [4]. According to Norimoto *et al.* [23], the internal damping described by $\tan\delta$ arises from a time lag between the deformation

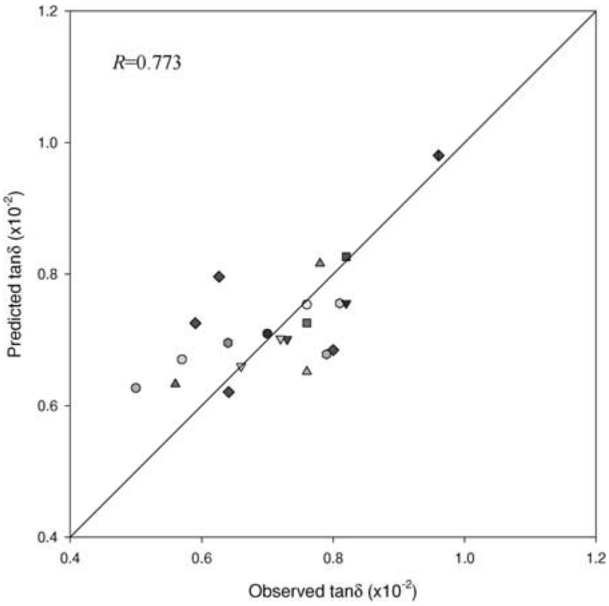

Figure 3 Multiple regression analysis plots. Criterion variable; $\tan\delta$, predictor variable; average crystal width (CW_{av}), MFA in earlywood (MFA_{EW}), proportion of latewood (P_{LW}). Symbols as in Fig. 2.

of the crystalline microfibril and the amorphous embedding matrix in the S_2 layer. Therefore, the negative correlation with crystalline parameters seems to imply an important contribution of the matrix components to $\tan\delta$.

Although multiple regression analysis is a very useful method to identify the possible structural parameters of significance, wood architecture is so complicated that it is difficult to select only a few factors to account for acoustic properties. The results obtained in this study should be considered as relating to but one of a number of possible influencing factors. In fact, some reports have already demonstrated that there are interactions between chemical components and physical or crystallographic properties [24–26]: for instance, Yano *et al.* [24, 25] demonstrated that alkali extraction possibly affects $\tan\delta$. Moreover, Saka and Tsuji [26] described a positive correlation between lignin concentration and MFA in the S_2 layer. Therefore, other factors relating to non-cellulosic constituents of cell walls should be considered.

4. Conclusions

We investigated crystallographic and anatomical features of 12 softwood samples. E/ρ has a strong negative correlation with MFAs both in earlywood and latewood, and a positive one with CW_{av}, while $\tan\delta$ has strong positive correlation with MFA in earlywood and P_{LW}, and a negative one with CW_{av}.

Sitka spruce was found to be quite distinct among the softwood species investigated. Sitka spruce wood is being regarded as one of the best acoustic materials for soundboards. Not only does it have a very low microfibril angle but the difference between MFA_{LW} and MFA_{EW} is very small. This has been similarly reported for *P. abies* [9], which is known as the best soundboard material. Even though there is no doubt that the averaged MFA is a factor that influences acoustic properties, the difference between MFA_{LW} and MFA_{EW} ought also to be taken into account. If this difference is small, the velocity of sound is more homogeneous in radial direction, i.e., across an annual ring.

In conclusion, relatively low and similar MFAs in both late- and earlywood are advantageous attributes of to be used wood for soundboards for the musical instruments.

Acknowledgment

The study was supported in part by Grant-in-Aid for Scientific Research from the Japan Society for the Promotion of Science (no. 12660151). We would like to thank the ESRF staff at the Microfocus Beamline, in particular Dr. Manfred Burghammer and Dr. Christian Riekel, for help with the synchrotron X-ray experiments.

References

1. T. ONO and M. NORIMOTO, *Jpn. J. Appl. Phys.* **22** (1983) 611.
2. *Idem.*, *Rheol. Acta* **23** (1984) 652.
3. T. ONO, *J. Acoust. Soc. Jpn.* **17** (1996) 4.
4. Y. KUBOJIMA, T. OKANO and M. OHTA, *Mokuzai Gakkaishi* **43** (1997) 634.
5. D. FENGEL and G. WEGENER, in "Wood" (Walter de Gruyter, Berlin, 1984) p. 13.
6. D. R. COWDREY and R. D. PRESTON, *Proc. Roy. Soc.* B **166** (1966) 245.
7. I. D. CAVE, *Wood Sci. & Technol.* **2** (1968) 268.
8. M. HERMAN, P. DUTILLEUL and T. AVELLA-SHAW, *IAWA J.* **20** (1999) 3.
9. H. F. JAKOB, P. FRATZL and S. E. TSCHEGG, *J. Struct. Biol.* **113** (1994) 13.
10. A. REITERER, H. LICHTENEGGER, S. E. STANZL-TSCHEGG and P. FRATZL, *Phil. Mag.* A **79** (1999) 2173.
11. H. LICHTENEGGER, A. REITERER, S. E. STANZL-TSCHEGG and P. FRATZL, *J. Struct. Biol.* **128** (1999) 257.
12. H. LICHTENEGGER, M. MÜLLER, O. PARIS, C. RIEKEL and P. FRATZL, *J. Appl. Cryst.* **32** (1999) 1127.
13. T. YANO and T. YAMADA, *Mokuzai Gakkaishi* **31** (1985) 222.
14. A. P. HARMMERSLEY, S. O. SVENSSON and A. THOMPSON, *Nucl. Instr. Meth.* A **346** (1994) 312.
15. M. MÜLLER, R. HORI, T. ITOH and J. SUGIYAMA, *Biomacromolecules* **3** (2002) 182.
16. P. SCHERRER, *Göttinger Nachr.* **2** (1918) 98.
17. E. MORK, *Papier Fabrikant.* **26** (1928) 741.
18. C. L. LEE, *Forest Prod. J.* **22** (1961) 108.
19. E.-L. HULT, P. T. LARSSON and T. IVERSEN, *Cellulose* **7** (2000) 35.
20. K. OKANO, T. SATO and S. HIRAI, *Mokuzai Gakkaishi* **15** (1969) 62 (in Japanese).
21. N. SOBUE, N. HIRAI and I. ASANO, *Mokuzai Gakkaishi* **16** (1970) 263 (in Japanese).
22. R. N. FORTHOFER and E. S. LEE, in "Introduction to Biostatistics" (Academic Press, San Diego, 1995) p. 438.
23. M. NORIMOTO, F. TANAKA, T. OHOGAMA and R. IKIMUNE, *Mokuzaikenkyu Shiryo* **22** (1986) p. 53 (in Japanese).
24. H. YANO, *Holzforschung* **48** (1994) 491.
25. H. YANO, H. KAJITA and K. MINATO, *J. Acoust. Soc. Am.* **96** (1994) 3380.
26. S. SAKA and M. TSUJI, *Cellulose Chem. Technol.* **21** (1987) 225.

Received 13 March
and accepted 8 July 2002